Distributed Strategy for Optimal Dispatch of Unbalanced Three-Phase Islanded Microgrids

Vergara Barrios, Pedro Pablo ; Rey-López, Juan Manuel; Shaker, Hamid Reza; Guerrero, Josep M.; Jørgensen, Bo Nørregaard; da Silva, Luiz Carlos Pereira

Published in:
IEEE Transactions on Smart Grid

DOI:
10.1109/TSG.2018.2820748

Publication date:
2019

Document version:
Accepted manuscript

This article has been accepted for publication in a future issue of this journal, but has not been fully edited. Content may change prior to final publication. Citation information: DOI 10.1109/TSG.2018.2820748, IEEE Transactions on Smart Grid

Distributed Strategy for Optimal Dispatch of Unbalanced Three-Phase Islanded Microgrids

Pedro P. Vergara, Juan M. Rey, Hamid R. Shaker, Josep M. Guerrero, *Fellow*, *IEEE*, Bo N. Jørgensen, Luiz C. P. da Silva.

***Abstract*—This paper presents a distributed strategy for the optimal dispatch of islanded microgrids, modeled as unbalanced three-phase electrical distribution systems (EDS). To set the dispatch of the distributed generation (DG) units, an optimal generation problem is stated and solved distributively based on primal-dual constrained decomposition and a first-order consensus protocol, where units can communicate only with their neighbors. Thus, convergence is guaranteed under the common convexity assumptions. The islanded microgrid operates with the standard hierarchical control scheme, where two control modes are considered for the DG units: a voltage control mode (VCM), with an active droop control loop, and a power control mode (PCM), which allows setting the output power in advance. To assess the effectiveness and flexibility of the proposed approach, simulations were performed in a 25-bus unbalanced three-phase microgrid. According to the obtained results, the proposed strategy achieves a lower cost solution when compared with a centralized approach based on a static droop framework, with a considerable reduction on the communication system complexity. Additionally, it corrects the mismatch between generation and consumption even during the execution of the optimization process, responding to changes in the load consumption, renewable generation and unexpected faults in units.**

***Index Terms*—Consensus algorithm, distributed dispatch, optimal power flow, nonlinear programming, three-phase microgrid.**

NOTATION

Sets:

$\mathcal{F}$	Set of phases {A, B, C}
$\mathcal{G}$	Set of DG units, $\mathcal{G} = \mathcal{G}_1 \cup \mathcal{G}_2$
$\mathcal{G}_1$	Set of DG units operating in PCM, $\mathcal{G}_1 \subset \mathcal{G}$
$\mathcal{G}_2$	Set of DG units operating in VCM, $\mathcal{G}_2 \subset \mathcal{G}$
$\mathcal{L}$	Set of lines
$\mathcal{N}$	Set of nodes of the EDS
$\mathcal{O}_m$	Set of operational constraints of the DG unit m
$\mathcal{W}$	Set of wind turbines (WTs) units

Indexes:

ϕ, ψ	Phases $\phi \in \mathcal{F}$ and $\psi \in \mathcal{F}$
mn	Line $mn \in \mathcal{L}$
m, n	Node $m \in \mathcal{N}$ and $n \in \mathcal{N}$

Parameters:

α_m	Constant parameter associated to the DGs operation cost
β_m	Linear parameter associated to the DGs operation cost
Δt_D	Length for the discretization of the operational time
$\Delta\omega$	Angular frequency deviation
ΔV	Voltage magnitude deviation
D_m^P	Active power droop gain of DG units in VCM
D_m^Q	Reactive power droop gain of DG units
ε	Parameter to control the converge of the active droop protocol
$\hat{\varepsilon}$	Parameter to control the converge of the frequency reference protocol
γ_m	Quadratic parameter associated to the DGs operation cost
λ	Dual variable associated with the active power balance constraint
λ_m	Local estimation of λ by the DG unit m
κ	Parameter to control the converge of consensus protocol
P_m^W	Expected active power generation of the WTs
$\overline{P}_m^G$	Maximum active generation limit of the DG units
$\underline{P}_m^G$	Minimum active generation limit of the DG units
$P_{m,\phi}^D$	Active load consumption
$\overline{Q}_m^G$	Maximum reactive generation limit of the DG units
$\underline{Q}_m^G$	Minimum reactive generation limit of the DG units
$Q_{m,\phi}^D$	Reactive load consumption
$\overline{V}$	Maximum voltage magnitude
$\underline{V}$	Minimum voltage magnitude
V_0	Nominal voltage magnitude
ω_0	Nominal angular frequency
ω_m	Frequency reference of the DG units in VCM
$Z_{mn,\phi,\psi}$	Line impedance
$Z'_{mn,\phi,\psi}$	Transformed line impedance, defined as $Z'_{mn,\phi,\psi} = Z_{mn,\phi,\psi} \angle \theta_\psi - \theta_\phi$

Continuous Variables:

P_m^G	Total active output power of the DG units
$P_m^{G_0}$	Total scheduled active of the DG units
$P_{mn,\phi}$	Active power flow in line mn at phase ϕ
Q_m^G	Total reactive generation power of the DG units

This work was supported by the São Paulo Research Foundation (FAPESP). Research Grants: 2015/09136-8 and 2016/04164-6.

Pedro P. Vergara and Luiz C. P. da Silva are with the Department of Systems and Energy, UNICAMP, University of Campinas, 13083-852 Campinas, São Paulo, Brazil (emails: {pedropa,lui}@fee.dsee.unicamp.br).

Juan M. Rey is with Escuela de Ingenierías Eléctrica, Electrónica y de Telecomunicaciones (E3T), Universidad Industrial de Santander (UIS), 680002 Bucaramanga, Colombia (e-mail: juanmrey@uis.edu.co).

Josep M. Guerrero is with the Department of Energy Technology, Aalborg University, Aalborg DK-9220, Denmark (e-mail: joz@et.aau.dk).

Pedro P. Vergara, Hamid R. Shaker and Bo N. Jørgensen are with the Center for Energy Informatics, University of Southern Denmark, Odense DK-5230, Denmark (emails: {pvb,hrsh,bnj}@mmmi.sdu.dk).

This article has been accepted for publication in a future issue of this journal, but has not been fully edited. Content may change prior to final publication. Citation information: DOI 10.1109/TSG.2018.2820748, IEEE Transactions on Smart Grid

$Q_{mn,\phi}$	Reactive power flow in line mn at phase ϕ
$S_{mn,\phi}$	Apparent power of line mn at phase ϕ
$S^{L}_{mn,\phi}$	Apparent power losses in line mn at phase ϕ
$V_{m,\phi}$	Voltage magnitude of nodes
ω	Frequency of the system

Remark: Through the paper, it is assumed that the DG unit $m \in \mathcal{G}$ (and equivalently the WT $m \in \mathcal{W}$), it is connected to the node $m \in \mathcal{N}$ of the EDS.

I. Introduction

TRADITIONALLY, the optimal dispatch of a microgrid is performed in a centralized way, where a system operator gathers all the operational and technical information of the distributed generation (DG) units, aiming to define the generation dispatch that minimizes the overall cost [1]. Centralized optimal strategies for microgrids have been proposed in [2]–[4]. Due to the way information is exchanged with the central operator, these approaches require high bandwidth communication infrastructures and high-levels of connectivity, increasing the complexity of their implementation, specially considering that the number of DG units can be large. Moreover, these approaches do not show privacy preserving characteristics, considering that units can belong to different owners, which might not be interested in sharing private operational information. In contrast, distributed approaches offer features that make them an interesting alternative, including scalability, adaptability, privacy preserving and robustness, allowing to respond to changes in the number of operating units, unexpected increase in renewable generation or load consumption, among others [5].

Recently, distributed approaches have drawn a lot of attention in the technical literature [6]. In general, two main groups can be identified: *(i)* the approaches based on consensus algorithms and *(ii)* the approaches based on local updating rules. In all these, the objective is to define the generation dispatch of each DG unit locally, limiting the amount of information that is exchanged between the DG units.

For the first group, in [7] an iterative algorithm is developed based on the incremental cost principle. This correspond to the consensus variable. In these works, a DG leader unit is required to balance the generation and load consumption. In [8], two consensus algorithms are executed in parallel to estimate locally the mismatch between generation and load consumption. In [9], a term is added to the consensus algorithm using only local information based on the nodal power balance equation, which plays the role of a gradient. In [10], [11] a modified consensus algorithm with finite-time convergence characteristics is presented, while in [12] a distributed gradient-based algorithm is developed, taken the derivative of the cost function of each DG unit as the consensus variable.

In the second group, simple updating rules are developed. These rules are continuously executed in an iterative procedure aiming to define the operational schedule of each unit until a convergence criterion is reached. For instance, in [13]–[17], the iterative rule is defined to be proportional to the active power mismatch between generation and load consumption. In addition to this, in [14], a proportional term based on the marginal cost is also considered. Thus, units with low marginal cost will increase their output power faster than high cost generators. As the active power mismatch is a global variable, and to be able to estimate it locally, in [13] local measurements of frequency deviation are used, while in [14] and [17], a complex communication procedure between neighbor units is considered.

The main drawback of the above-discussed works [7]– [17], is that they assume that all the generators and loads are connected to one bus, ignoring the underlying operation of the electrical distribution system (EDS). In general, in these works it is assumed that a balancing mechanism operates i. e., a leader unit supply the required active power to correct the mismatch between generation and load consumption; all this while the optimization algorithm is executed. In an actual operation, this is not a practical assumption since the mismatch between the generation and load consumption is corrected in a faster speed of response (normally, in the order of seconds) by the lower level controllers [18]. Moreover, as in islanded operation the DG units are responsible for providing the frequency and voltage magnitude references for the system, if the optimal dispatch does not consider the control operation of the DG units, the system might operate with a higher frequency or voltage deviation, and consequently, the optimal schedule might not be technically feasible. In this regard, in [5], [19], a distributed approach including the operation of the EDS was developed. However, a centralized communication infrastructure is still required, while the unbalanced operation of the microgrid is not taken into account.

Considering this, a distributed strategy for the optimal dispatch of islanded microgrids is presented in this paper. The microgrid is modeled as an unbalanced three-phase EDS, operating within a hierarchical control scheme. To define the active dispatch of the DG units, an optimal generation problem is stated and solved distributively using a first-order consensus protocol, where units can communicate only with their neighbors. This strategy is based on primal-dual constrained decomposition theory, in order to distribute the problem among the units and take into account locally their technical operational requirements. Thus, convergence is guaranteed under the common convexity assumptions. Additionally, two control modes are considered for the DG units: a voltage control mode (VCM), with an active droop control loop, and a power control mode (PCM), which allows setting the output power of the unit in advance. To assess the effectiveness and flexibility of the proposed approach, simulations were performed in a 25-bus microgrid for different case of studies. According to the results, the proposed strategy achieves a lower cost solution when compared with a centralized approach, with a considerable reduction on the communication system complexity, responding to changes in the load consumption, renewable generation, and unexpected faults in units.

Among all the features previously discussed of the proposed distributed strategy, the main contributions of this paper can be summarized as follows:

- The proposed strategy considers the control modes of the DG units (VCM and PCM) in the optimization

This article has been accepted for publication in a future issue of this journal, but has not been fully edited. Content may change prior to final publication. Citation information: DOI 10.1109/TSG.2018.2820748, IEEE Transactions on Smart Grid

approach. In this context, as the units in VCM operate with a droop control loop, these are responsible for correcting the active power mismatch between generation and consumption after any load or renewable generation increase/decrease, and more importantly, during the execution of the optimization algorithm.

- The proposed strategy is considered to operate within the standard hierarchical control framework for microgrids. Thus, it is ensured that the dynamics of the optimization algorithm and the primary control layer (implemented with droop control) are decoupled, which helps to maintain the stability of the system. Moreover, it considers a correction protocol, in order to operate in steady-state with a lower frequency deviation.

II. Control and Operation of Microgrids

Microgrids can operate in two modes: grid-connected or islanded mode. In grid-connected mode, the frequency and voltage magnitude references are provided by the main grid, while in islanded mode, these must be provided by the DG units [20]. Since the operation of microgrids deals with issues from different technical areas, time scales and infrastructure levels, the hierarchical control scheme has been widely accepted as the standard solution [18].

In general, the hierarchical control scheme comprises three different and well defined levels: (*i*) a primary level, the fastest level, responsible for the local control of the DG units, generally based on droop control, which does not require communications; (*ii*) a secondary level, which deals with the deviation at steady-state conditions of the frequency and the voltage magnitude due to the operation of the primary level; and (*iii*) a tertiary level, the slowest level, responsible for the economical operation of the system, implemented through a dispatch algorithm, generally based on the solution of an optimization problem.

A. Primary and Secondary Control Level

Regarding the primary control level, DG units can operate in two different control modes: power control mode (PCM) and voltage control mode (VCM) [21]. In islanded operation, at least one unit is required operating in VCM to define the frequency and voltage magnitude reference of the EDS [18]. Hence, if the unit operates in PCM, the output power can be set at the schedule value defined by the tertiary control level, i.e.,

$$P_m^G = P_m^{G_0}, \quad \forall m \in \mathcal{G}_1. \tag{1}$$

In this case, the output power is independent of the state of the EDS. Different from this, if the unit operate in VCM, its output power cannot be set in advance, since this unit operates with a droop control loop. Therefore, all units in VCM share the remaining active power mismatch between generation and consumption, in inverse proportion to their active droop gain (D_m^P). The droop operation of a unit in VCM mode can be represented using the expression,

$$\omega = \omega_m - D_m^P P_m^G, \quad \forall m \in \mathcal{G}_2, \tag{2}$$

where P_m^G is the total active output power of the unit. A schematic representation of both control modes is shown in Fig. 1. The droop gain D_m^P reflects the slope of the $\omega - P$ curve. Thus, the total output power of units in VCM (i.e., P_m^G) can be set to their scheduled value ($P_m^{G_0}$), tuning D_m^P; all this in order to minimize the overall generation cost.

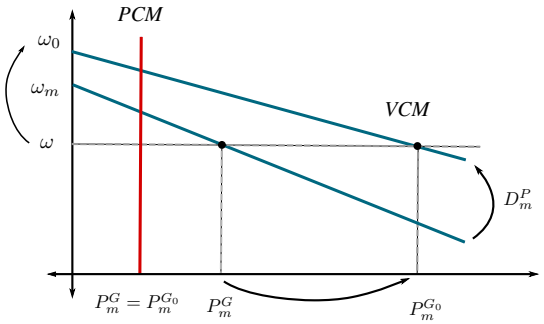

Figure 1. Control modes of the DG units: VCM and PCM. The line in the VCM indicates the direction of variation in P_m^G when D_m^P is decreased. Additionally, ω_m can be modified in order to reduce the frequency deviation.

The main difference between these control modes is related to the operation of the control loops and how these set the output power in steady-state conditions. Thus, they are essentially independent, which means that each DG unit can decide its operation mode (see Sec. IV-C for a further discussion). Implementation and stability issues related to the transition between both control modes are discussed in detail in [21].

As for the reactive power Q_m^G, in both control modes all the DG units share the reactive power consumption defining their output voltage magnitude using the expression,

$$V_{m,\phi} = V_0 - D_m^Q Q_m^G, \quad \forall m \in \mathcal{G}. \tag{3}$$

This droop control is based on the assumption that the output impedance of the DG unit is inductive, which is valid for synchronous-based and the majority of inverted-based units, coupled to the EDS with an inductor filter. Nevertheless, in case of output non-inductive impedance, control strategies that aims to decouple the active and reactive power regulation can be implemented, e.g. virtual output impedance strategies [22].

Regarding the secondary control level, its main function is related to the definition of the frequency and voltage reference i. e., ω_m and V_0. This is done in order to reduce the frequency and voltage deviation in steady-state conditions [23], and as shown in Fig. 1. The operation of the secondary control level can be seen as a correction process, which operates with a lower speed of response than the primary control, in order to maintain their dynamics decoupled.

B. Tertiary Control Level

Regarding the tertiary level, to define the operational schedule of the DG units, an optimization problem is formulated and solved. The formulation of this problem must account for all the operational constraints of units, while the total load consumption is supplied with minimum generation cost. In general, this problem is known as the optimal generation problem, which can be stated using the formulation given by (4)–(6), for a microgrid comprising DG units, WT units and loads.

$$\min_{P_m^{G_0}, \forall m \in \mathcal{G}} \left\{ \sum_{m \in \mathcal{G}} f_m(P_m^{G_0}) \right\} \tag{4}$$

This article has been accepted for publication in a future issue of this journal, but has not been fully edited. Content may change prior to final publication. Citation information: DOI 10.1109/TSG.2018.2820748, IEEE Transactions on Smart Grid

subject to,

$$\sum_{m\in\mathcal{G}} P_m^{G_0} + \sum_{m\in\mathcal{W}} P_m^W = \sum_{m\in\mathcal{N}}\sum_{\phi\in\mathcal{F}} P_{m,\phi}^D \tag{5}$$

$$\underline{P}_m^G \le P_m^{G_0} \le \overline{P}_m^G \quad \forall m \in \mathcal{G}. \tag{6}$$

In the above formulation, the objective function in (4) aims to minimize the overall generation cost, where $f_m(P_m^{G_0})$ models the generation cost of each DG unit, which can be approximated with a quadratic function [1], such as,

$$f_m(P_m^{G_0}) = \gamma_m(P_m^{G_0})^2 + \beta_m P_m^{G_0} + \alpha_m, \quad \forall m \in \mathcal{G}, \tag{7}$$

where usually γ_m holds a positive value, which yields convexity of the generation cost function.

For the operational constraints, the active power balance in the EDS (neglecting power losses) is modeled in (5), as a function of the three-phase output power of the DG units (P_m^G), WT units (P_m^W) and the load consumption ($P_{m,\phi}^D$); while constraints in (6) models the generation limits of the DG units.

III. Distributed Optimal Strategy

In this section, a description of the communication topology of the DG units seen as a graph is discussed. Additionally, the consensus algorithm used is introduced. Then, the distributed optimal strategy is presented. Finally, an overview of the proposed approach is discussed.

A. First-Order Consensus Algorithm

Let the graph $G = (\mathcal{V}, \mathcal{E}, A)$ describes the communication topology of the DG units. For this graph, the set of nodes $\mathcal{V}$ represents the set of DG units, while the set of edges $\mathcal{E} \subset \mathcal{V}\times\mathcal{V}$ represents the set of communication links between the DG units. Considering this, an adjacency matrix $A = [a_{mn}]$, with non-negative adjacency elements a_{mn}, can be defined for the microgrid. The adjacency elements associated with the communication links (or edges of the graph) are positive, i.e., $a_{mn} = 1\ \forall(m,n) \in \mathcal{E}$, and otherwise, $a_{mn} = 0$. Additionally, $\mathcal{N}_m$ is defined as the set of neighbors of the DG unit m, i.e., the set of DG units that can exchange information with unit m. Finally, the cardinality (i.e., the size) of the set $\mathcal{N}_m$ is deifned as $\overline{d}_m$.

Define for the DG unit m a generic variable $x_m \in \mathbb{R}$, and named it as the consensus variable. The consensus variable represents the quantity in which all the DG units want to agree (in Sec. III-B, the consensus variable defined corresponds to λ, i.e., the incremental cost variable). Thus, it can be said that the DG unit m and n agree if and only if $x_m = x_n$. Moreover, it can be said that all the DG units have reached consensus if and only if $x_m = x_n\ \forall m, n \in \mathcal{V}$.

The dynamics of the consensus variable x_m for each DG unit can be described by the discrete-time model in (8), where k is an iteration counter.

$$x_m(k+1) = x_m(k) + u_m(k). \tag{8}$$

It can be shown that under the protocol in (9), all the DG units reach consensus when $k \to \infty$ [24], where $C = [c_{mn}]$ is known as the consensus matrix.

$$u_m(k) = \sum_{n\in\mathcal{N}_m} c_{mn}(x_n(k) - x_m(k)). \tag{9}$$

Thus, after replacing (9) into (8), and some re-arrange, the dynamics of the consensus variable of each DG unit can be updated using (10), which can be seen as the weighted average of its current state and the current state of its neighbors units.

$$x_m(k+1) = \sum_{n\in\mathcal{N}_m} c_{mn}x_n(k). \tag{10}$$

To reach consensus under dynamics in (10), the consensus matrix $C = [c_{mn}]$ can be defined as [14],

$$c_{mn} = \begin{cases} 1/(\overline{d}_m + 1) & \text{if } n \in \mathcal{N}_m \cup \{m\}, \\ 0 & \text{if } n \notin \mathcal{N}_m. \end{cases} \tag{11}$$

Such definition leads to a row-stochastic (i.e., row sum of 1), as required according [25]. It is important to highlight that the notion of neighborhood used here is related to the existence of a communication link between the DG units. The protocol in (10) is known as the first-order consensus algorithm, and its speed of convergence depends on the level of connectivity of the communication topology of the DG units. Nevertheless, convergence is guarantee as long as the communication topology fulfills the design requirements discussed in Sec. III-E.

B. Distributed Optimal Dispatch Strategy

The optimal generation problem, as formulated in Section II-B, can be solved using a distributed optimization approach taking advantage of its structure. In this, the only constraint that couple the problem among all the units is the active power balance in (5). Moreover, the set of operational constraints of the DG units, given by (6), defines a closed and convex set[1] $\mathcal{O}_m, \forall m \in \mathcal{G}$, in such a way that $\mathcal{O}_m \cap \mathcal{O}_n = \emptyset, \forall m, n \in \mathcal{G}$; or in other words, the operational constraints of the DG unit m are independent of those of unit n. In this case, only generation limit constraints are considered. However, other operational constraints such as prohibited operational zones can be added to the set $\mathcal{O}_m$ without modifying the proposed optimization strategy.

Based on this, a distributed strategy can be developed. Firstly, define the Lagrangian function $L(P_m^{G_0}, \lambda)$ as

$$L(P_m^{G_0}, \lambda) = \sum_{m\in\mathcal{G}} f_m(P_m^{G_0}) + \lambda\left(\sum_{m\in\mathcal{N}}\sum_{\phi\in\mathcal{F}} P_{m,\phi}^D - \sum_{m\in\mathcal{G}} P_m^{G_0} - \sum_{m\in\mathcal{W}} P_m^W\right), \tag{12}$$

where λ corresponds to the dual variable associated to constraint in (5). The optimal solution, which defines the active power dispatch of each DG unit, must meet the first optimality condition, which can be expressed as

$$\frac{\partial L(\cdot)}{\partial P_m^{G_0}} = \frac{df_m(P_m^{G_0})}{dP_m^{G_0}} - \lambda = 0, \qquad \forall m \in \mathcal{G} \tag{13}$$

or equivalently [26],

$$\min_{P_m^{G_0}\in\mathcal{O}_m} \left[f_m(P_m^{G_0}) - \lambda P_m^{G_0}\right]. \tag{14}$$

[1]Notice that $\mathcal{O}_m$ as defined in (6), is closed due that P_m^G take values within the range $\underline{P}_m^G \le P_m^G \le \overline{P}_m^G$. Additionally, it is convex since it is described by a set of linear equations.

This article has been accepted for publication in a future issue of this journal, but has not been fully edited. Content may change prior to final publication. Citation information: DOI 10.1109/TSG.2018.2820748, IEEE Transactions on Smart Grid

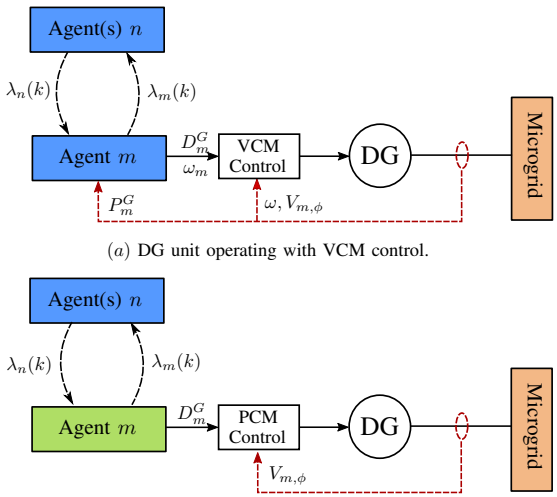

(a) DG unit operating with VCM control.

(b) DG unit operating with PCM control.

Figure 2. Structure of a DG unit seen as an agent. The black dashed lines represent exchange of information between different agents, while the red dashed lines represent local measurements.

Therefore, to define its scheduled active power, i.e., $P_m^{G_0}$, each DG unit $m \in \mathcal{G}$ solve (14) locally. The only global information required to solve (14) corresponds to λ, which can be estimated locally by each unit. To do this, variable λ_m is introduced and defined as the local estimation of the dual variable by unit m. From the economic operation of power systems, λ_m can be seen as the incremental cost of the DG units. Hence, the minimum cost dispatch is reached when all units have the same incremental cost value [7]. This condition is equivalent to state that $\lambda_m = \lambda_n, \forall m, n \in \mathcal{G}$, which suggests that variable λ_m can be defined as the consensus variable. Therefore, to estimate λ_m, this paper proposes that each unit execute locally the iterative consensus protocol given by,

$$\lambda_m(k+1) = \sum_{n \in \mathcal{N}_m} c_{mn}\lambda_n(k) + \kappa(P_m^G - P_m^{G_0}),\ \forall m \in \mathcal{G}, \quad (15)$$

where κ is a parameter that controls the convergence of the protocol. Notice that for units operating in PCM, the second term in (15) is reduced to zero, due to (1). The rationale of protocol in (15) can be understood if each DG unit is modeled as an independent agent, with functionalities such as acquiring local measurements, exchange information with its neighboring agents and define its active power schedule independently. A representation of the structure and information flow of a DG unit as an agent for both control modes, is shown in Fig. 2.

Notice that each DG unit has two active power variables: P_m^G, which stands for the active output power, and $P_m^{G_0}$, which stands for the scheduled active output power. These two variables must not be confused: $P_m^{G_0}$ is obtained for all the DG units solving the problem in (14), and corresponds to the output power that minimizes the total generation cost, while P_m^G is the actual power that the DG unit is supplying to the microgrid. Thus, the active output power of a DG unit operating in PCM, can be directly set considering (1). On the other hand, as the output power of units operating in VCM cannot be directly set (i.e., P_m^G cannot take directly the value given by $P_m^{G_0}$), the active droop gain (D_m^P) is modified iteratively using the protocol,

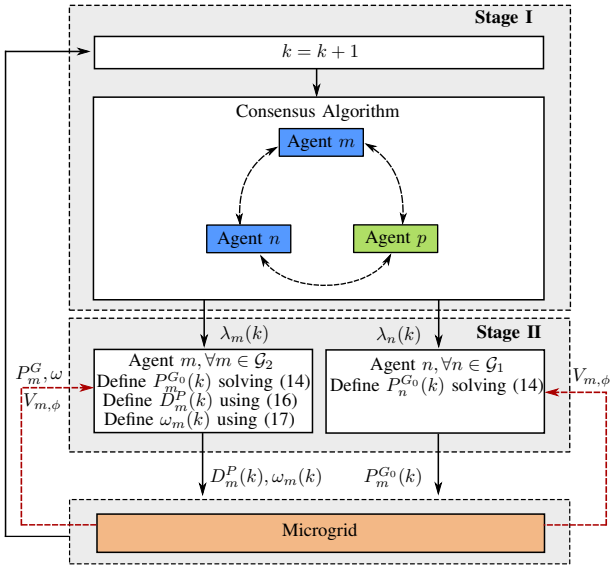

Figure 3. Flowchart of the proposed distributed dispatch strategy composed of Stage I and Stage II.

$$D_m^P(k+1) = D_m^P(k) + \varepsilon(P_m^G - P_m^{G_0}),\ \forall m \in \mathcal{G}_2, \quad (16)$$

where ε controls the convergence. This protocol guarantees that the active output power of the DG units in VCM (P_m^G), defined through the droop expression in (2), equals the dispatched power ($P_m^{G_0}$), defined cooperatively by all the DG units.

Nevertheless, when D_m^P is modified, the system might reach a steady-state with a frequency different from the nominal frequency value, given by ω_0. To reduce this deviation, each unit updates its frequency reference (ω_m) in (2), using the following protocol,

$$\omega_m(k+1) = \omega_m(k) + \hat{\varepsilon}(\omega_0 - \omega),\ \forall m \in \mathcal{G}_2. \quad (17)$$

This protocol guarantees that the system will operate with a lower frequency deviation in steady-state. A theoretical convergence analysis of protocols (15), (16) and (17), is presented in the Appendix.

As for the reactive power, and as shown in Fig. 2, information about the voltage at the node of connection is required for all units in order to define their reactive output power using (3). In this case, reactive power has not been considered in the optimization strategy, as it does not incur in any cost [27].

C. Overview of the Distributed Strategy

Fig. 3 shows the flowchart of the proposed distributed dispatch strategy, composed of two stages: one to run the consensus protocol (Stage I) and other to run the optimization algorithm (Stage II). At each iteration k, each stage can be explained as follows:

Stage I: All DG units execute locally their consensus protocols, as explained in Section III-B, in order to calculate $\lambda_m(k)$, i.e., the local estimation of variable λ. Here, it is assumed that the exchange of information between the DG units is done synchronously, i.e., the time-delay of the communication process is not considered. Additionally, recall that the exchange of information between units depends on the

This article has been accepted for publication in a future issue of this journal, but has not been fully edited. Content may change prior to final publication. Citation information: DOI 10.1109/TSG.2018.2820748, IEEE Transactions on Smart Grid

communication topology, as explained in Sec. III-A and shown in Fig. 3.

Stage II: Here, each DG unit solves the problem in (14) independently, in order to define $P_m^{G_0}(k)$, i.e., the optimal dispatch that minimizes the overall generation cost for the current $\lambda_m(k)$. To be able to solve the sub-problem in (14), each DG unit requires: $\lambda_m(k)$ (previously calculated in the Stage I), and its own operational data i.e., parameters of the cost function $(\alpha_m, \beta_m, \gamma_m)$, maximum and minimum active generation capacity $(\underline{P}_m, \overline{P}_m)$. Additionally, the units in VCM update their parameters $D_m^P(k)$ and $\omega_m(k)$, using (16) and (17), respectively.

It is important to highlight that, as the consensus protocol of units operating in VCM considers the current output power though the droop control loop, the proposed strategy takes into account the active power losses, even if these were not considered in the formulation stated in Sec. II-B.

Notice that, in order to update protocols (16) and (17) in Stage II, operational information of the EDS, such as the frequency (ω) and the current output power of the DG units in VCM (P_m^G), is required (see Fig. 2). This information can be obtained by the DG unit through local measurements, as explained in [12].

D. Operation within the Hierarchical Control Framework

To better understand the operation of the proposed strategy within the hierarchical control scheme, consider the illustrative example of the dynamics of the microgrid shown in Fig. 4. The hierarchical control is activated at t_1. Before this time it is considered that the microgrid is in steady-state operation, and the DG unit m has output power P_m^G. After t_1, the active droop gain D_m^P is modified, forcing the unit in VCM to supply $P_m^{G_0}$ (previously defined as a predetermined value of the tertiary control). This process is performed by the primary control level, which operates with the fastest time of response, denominated as $\mathcal{T}_P$. Due to the operation of the primary control, the frequency is modified, as shown in Fig. 4*b*. This frequency deviation is corrected by the secondary level, which acts in a slower time scale compared with the primary level. For this reason, its time of response $\mathcal{T}_S$ is greater than $\mathcal{T}_P$, which helps to decouple its dynamics. Finally, the tertiary level operates defining the new scheduled active power value $P_m^{G_0}$ with the slowest time scale $\mathcal{T}_T$. Thus, the update of the dispatch variables is done once the frequency recovery process is completed.

In this context, considering the operation of the proposed distributed strategy, Stage I and II perform the functions of the tertiary and secondary control, defining the optimal schedule of all the DG units (i.e., $P_m^{G_0}$), as well as the parameters of the droop control to reduce the frequency deviation in steady-state conditions (i.e., D_m^P, ω_m). Considering this, and aiming to maintain decoupled the dynamics of Stage I and II and the primary control, the response time of the proposed strategy (named as $\mathcal{T}_D$ in Fig. 4*a*) should be selected to have a value greater than $\mathcal{T}_S$, but lower than $\mathcal{T}_T$, i.e., $\mathcal{T}_S \leq \mathcal{T}_D \leq \mathcal{T}_T$. The selected value will depend on the speed of response desired for the system. Usually, $\mathcal{T}_S$ takes values near to 30 s or lower [23], [28], [29], while $\mathcal{T}_T$ can take values between 5 to 15 minutes [18]. Notice also that $\mathcal{T}_D$ limits the maximum processing time of the proposed strategy in a practical implementation.

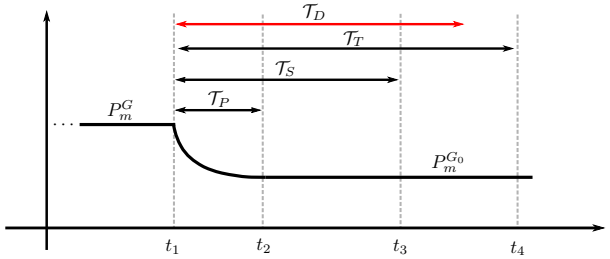

(a) Active output power of the DG unit m operating in VCM.

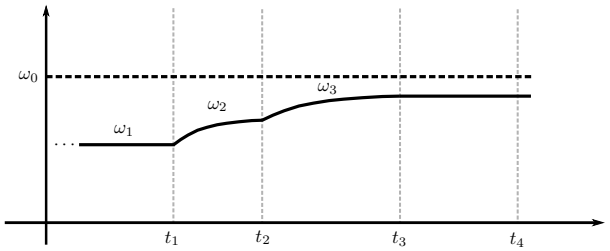

(b) Angular frequency of the microgrid.

Figure 4. Illustrative example of the dynamics of the primary, secondary and tertiary control level. The convergence time of the optimization algorithm in the proposed strategy is limited by the time length $\mathcal{T}_D$.

E. Design Considerations

The selection of the parameters κ, ε and $\hat{\varepsilon}$ in protocols, (15), (16) and (17), can affect the speed of convergence of the distributed strategy. Higher values for these parameters can lead to a faster convergence. However, a trade-off exists so that if they are set too large, an oscillatory behavior can be observed due to the excessively fast update of $\lambda_m(k)$ in (15). Additionally, the number of DG units also affects the choice of these parameters. It is possible to observe that, after a load or WT generation increase/decrease, the higher number of DG units in VCM, the lower the active power that each DG unit supply to reduce the mismatch between generation and load consumption; which means that the output power of the DG unit (P_m^G) might not be too far from its new schedule value ($P_m^{G_0}$). Therefore, the distributed approach can converge faster. This analysis suggests that the control parameters κ, ε and $\hat{\varepsilon}$ should be set inversely proportional to the number of DG units, N. Thus, the following heuristic rules can be used,

$$\kappa = 100/N, \quad \varepsilon = 1/100N, \quad \hat{\varepsilon} = 1/N. \tag{18}$$

Although these rules do not estimate an optimal value for the convergence parameters κ, ϵ and $\hat{\epsilon}$, these have shown a good performance in different scenarios, as described in Sec. IV-F.

The design of the communication topology can follow multiple criteria in order to define how the DG units exchange information, including: geographical localization, closeness in the electrical network, tolerance to links failure, among others [7], [12]. Nevertheless, the convergence of the distributed strategy is guarantee as long as the graph $\mathcal{G}$, that models the communication topology, meets, at least, the next design criteria:

This article has been accepted for publication in a future issue of this journal, but has not been fully edited. Content may change prior to final publication. Citation information: DOI 10.1109/TSG.2018.2820748, IEEE Transactions on Smart Grid

Table I
DG UNITS INFORMATION

m	γ_m[\$/kW^2]	β_m[\$/kW]	α_m[\$]	$\underline{P}^G_m$[kW]	$\overline{P}^G_m$[kW]	$\underline{Q}^G_m$[kvar]	$\overline{Q}^G_m$[kvar]
8	0.444	0.111	0.0	90	900	-180	540
13	0.264	0.067	0.0	150	1500	-300	900
19	0.400	0.100	0.0	120	1200	-120	720
22	0.500	0.125	0.0	80	800	-160	480
25	0.250	0.063	0.0	160	1600	-240	960

- There exists a path that links any DG unit m to any DG unit n. This condition guarantee that all the DG units are connected.
- The consensus matrix $C = [c_{mn}]$ is balanced, which can be obtained with bidirectional communications links.

The use of the proposed strategy, as based on a distributed approach, reduces the dependence on the communication system complexity when compared with a centralized approach. In fact, in a centralized approach, a high level of connectivity is required due to the central operator, reducing its robustness and reliability since a single point of failure exists. Moreover, in case of a link failure, the corresponding DG unit will be isolated, preventing its control. In this context, in the proposed strategy the communication topology can be designed to be robust in case of any link failure, following, for instance, the design rule presented in [12]. Additionally, as there is no leader unit, the system will continue its operation in case of a unit fault, as will be shown in Sec. IV-D.

IV. SIMULATION RESULTS AND DISCUSSION

The proposed strategy was tested in the unbalanced 25-bus microgrid shown in Fig. 5a. In total, five DG units and two WT units are considered. For comparison purposes, the two communication topology shown in Fig. 5 are considered. These are selected as they correspond to the more common topologies used in literature to test distributed algorithms [7]. Nevertheless, other topologies can be tested as well, as long as they meet the design requirements described in Sec. III-E.

The information of the DG units is shown in Table I. The reactive droop gain of all units were defined as in (19), while at initialization (i.e., at $k = 0$), the active droop gain of the units operating in VCM were defined as in (20). This definition allows the DG units operating in VCM achieve proper active power sharing according to their power ratings [30].

$$D^Q_m = (\overline{V} - \underline{V})/2\overline{Q}^G_m, \quad \forall m \in \mathcal{G} \tag{19}$$

$$D^P_m(k) = \Delta\omega/\overline{P}^G_m, \quad \forall m \in \mathcal{G}_2 | k = 0. \tag{20}$$

Additionally, $\underline{V}$, $\overline{V}$ and $\Delta\omega/2\pi$ were set to 0.94 p.u., 1.05 p.u. and 0.1 Hz, respectively. The parameter κ was set in 20, while ε and $\hat{\varepsilon}$ were defined to be 0.02 and 0.2, respectively, using (18). The active power in all the protocols is in *p.u.*, using 1000 kW as the nominal base. Initially, the WT units are not operating. The units G_{13}, G_{19}, G_{25} operate in VCM, while units G_8, G_{22} operate in PCM. The distributed model was implemented in AMPL and solved with IPOPT [31], using a computer with an Intel i7-4749 processor and 16 GB RAM.

As explained in Sec. III-C, at each iteration k, information related to the the frequency (ω) and the current output power

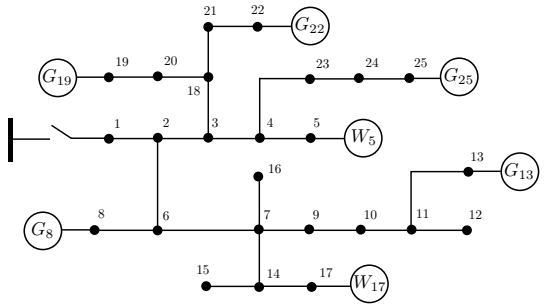

(a) 25-bus three-phase microgrid.

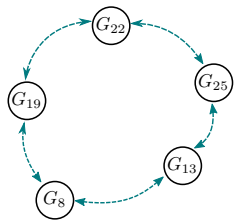

(b) Ring topology.

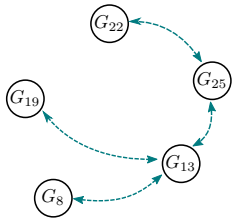

(c) Tree topology.

Figure 5. Microgrid and the communication topology presented as a graph. The data of the system and load demand of each node can be found in [32].

of the DG units in VCM (P^G_m) is required to update protocols (16) and (17). To simulate this measurement process, in this paper, an optimal power flow (OPF) formulation is used, as explained next in Sec. IV-A.

A. Simulation of the Measurement Process

In order to simulate the physical response of the microgrid during the optimization process at each iteration k, an optimal power flow formulation is solved. In practical cases, the response in the microgrid variables is measured using sensors locally implemented in each DG unit, thus, this formulation is not necessary.

The use of this formulation is based on two facts: first, the dynamics of the primary control level is faster than the dynamics of the higher control levels (or equivalently, $\mathcal{T}_D \gg \mathcal{T}_P$ in Fig. 4); and second, to define D^P_m in (16), P^G_m is obtained filtering the measured instantaneous active power with a low-pass filter [23]. This means that, at the end of the time length $\mathcal{T}_D$, the system has reached a steady-state condition, which can be estimated using a power flow model [30].

The unbalanced three-phase islanded OPF formulation is given by the non-linear optimization problem in (21)–(33), which is based on the work presented in [33]. Notice that in this formulation there are not control variables, thus, its solution is equivalent to the one provided by a three-phase power flow tool, such as OpenDSS or GridLabD.

$$\min \left\{ \sum_{mn \in \mathcal{L}} \sum_{\phi \in \mathcal{F}} \Re\{S^L_{mn,\phi}\} \right\}, \tag{21}$$

where $S^L_{mn,\phi}$ is defined as,

$$S^L_{mn,\phi} = \left(\sum_{\psi \in \mathcal{F}} \frac{Z'_{mn,\phi,\psi} S^*_{mn,\psi}}{V_{m,\phi} V_{m,\psi}} \right) S_{mn,\phi}. \tag{22}$$

This article has been accepted for publication in a future issue of this journal, but has not been fully edited. Content may change prior to final publication. Citation information: DOI 10.1109/TSG.2018.2820748, IEEE Transactions on Smart Grid

Subject to:

$$\sum_{lm\in\mathcal{L}} P_{lm,\phi} - \sum_{mn\in\mathcal{L}} \left(P_{mn,\phi} + \Re\{S^L_{mn,\phi}\}\right) + \sum_{m\in\mathcal{G}_1} P^{G_0}_m(k)/3 + \sum_{m\in\mathcal{G}_2} P^G_{m,\phi} = P^D_{m,\phi} - \sum_{m\in\mathcal{W}} P^W_m/3 \quad \forall m\in\mathcal{N}, \forall\phi\in\mathcal{F} \quad (23)$$

$$\sum_{lm\in\mathcal{L}} Q_{lm,\phi} - \sum_{mn\in\mathcal{L}} \left(Q_{mn,\phi} + \Im\{S^L_{mn,\phi}\}\right) + \sum_{m\in\mathcal{G}} Q^G_{m,\phi,t} = Q^D_{m,\phi} \quad \forall m\in\mathcal{N}, \forall\phi\in\mathcal{F} \quad (24)$$

$$V^2_{m,\phi} - V^2_{n,\phi} = 2\sum_{\psi\in\mathcal{F}} \Big(\Re\{Z'_{mn,\phi,\psi}\}P_{mn,\psi} + \Im\{Z'_{mn,\phi,\psi}\}Q_{mn,\psi}\Big) - \frac{1}{V^2_{m,\phi}}\left|\sum_{\psi\in\mathcal{F}} Z'^{*}_{mn,\phi,\psi}S_{mn,\phi}\right|^2 \quad \forall mn\in\mathcal{L}, \forall\phi\in\mathcal{F} \quad (25)$$

$$P^G_m = \sum_{\psi\in\mathcal{F}} P^G_{m,\psi} \quad \forall m\in\mathcal{G}_2 \quad (26)$$

$$Q^G_m = \sum_{\psi\in\mathcal{F}} Q^G_{m,\psi} \quad \forall m\in\mathcal{G} \quad (27)$$

$$\omega = \omega_m(k) - D^P_m(k)P^G_m \quad \forall m\in\mathcal{G}_2 \quad (28)$$

$$V_{m,\phi} = V_0 - D^Q_m Q^G_m \quad \forall m\in\mathcal{G} \quad (29)$$

$$V_{m,\phi} = V_{m,\psi} \quad \forall m\in\mathcal{G}_2, \forall\phi,\psi\in\mathcal{F} \quad (30)$$

$$\underline{V} \le V_{m,\phi} \le \overline{V} \quad \forall m\in\mathcal{N}, \forall\phi\in\mathcal{F} \quad (31)$$

$$\underline{P}^G_m \le P^G_m \le \overline{P}^G_m \quad \forall m\in\mathcal{G}_2 \quad (32)$$

$$\underline{Q}^G_m \le Q^G_m \le \overline{Q}^G_m \quad \forall m\in\mathcal{G} \quad (33)$$

In the above formulation, the objective function in (21) aims to minimize the total active power losses of the EDS. This ensure that the solution of the power flow formulation matches the steady-state operation of the unbalanced microgrid, considering the active droop loop of the DG units operating in VCM and the reactive droop loop of all units [30], [33]. The EDS is modeled by (23)–(25), derived as a function of the active and reactive power flow through lines, i.e., $S_{mn,\phi} = P_{mn,\phi} + jQ_{mn,\phi}$. The line impedance is considered to be constant. Additionally, a transformation is introduced and defined as $Z'_{mn,\phi,\psi} = Z_{mn,\phi,\psi}\angle\theta_\psi - \theta_\phi$. Notice that due to this definition $Z'_{mn,\phi,\psi}$ is not symmetric as $Z_{mn,\phi,\psi}$. Constraints (23) and (24) model the active and reactive power balance, respectively, considering the output power of the DG units operating in VCM and PCM, and the balanced power of the WTs.

In (23), the three-phase output power of DG units in PCM is modeled as a balanced constant power injection, which value was previously defined in the Stage II (i.e. $P^{G_0}_m(k)$, see Fig. 3); while the three-phase output power of units operating in VCM is considered as a power flow variable. Equation (25) models the voltage magnitude drop in the lines. In (26), the three-phase output power of units in VCM is modeled as a function of their output power per phase, while (27) models the three-phase reactive output power of all units (in PCM and VCM). The active droop expression of units in VCM is considered using (28), while the reactive droop expression is considered in (29) for all units (in PCM and VCM). Constraint in (30) models the electromotive force of synchronous-based DG units, which is represented by the balanced voltages magnitudes at their internal nodes [2]. Constraint in (31) enforces the maximum and minimum limits for the voltage magnitudes. Finally, the total active generation power limits are defined by (32) for units in VCM, while the total reactive generation limits are defined by (33) for all units. For a more detailed discussion of this power flow formulation and the DG units modeling, see [33].

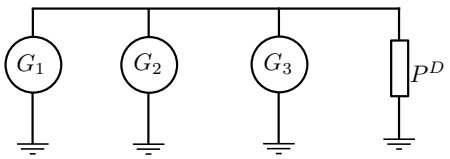

Figure 6. Microgrid used for the simple numerical example. DG units G_1 and G_2 operate in VCM, while the DG unit G_3 operate in PCM. The total load demand is defined to be 400 kW.

Table II
DG UNITS INFORMATION FOR THE NUMERICAL EXAMPLE

m	γ_m[\$/kW^2]	β_m[\$/kW]	α_m[\$]	$\underline{P}^G_m$[kW]	$\overline{P}^G_m$[kW]
1	0.20	0.25	0.0	40	400
2	0.50	0.15	0.0	20	200
3	0.30	0.22	0.0	25	250

B. Numerical Example

In order to illustrate the proposed strategy, a simple numerical case is presented in this section, applying the distributed approach, which is summarized in (40) to (45) in the Appendix. This simple case is composed of three DG units, the DG unit G_1 and G_2 operate in VCM, while the DG unit G_3 operates in PCM. The total load consumption is defined as 400 kW, while the system is considered to be lossless, as shown in Fig. 6. The DG units parameters are shown in Table II, meanwhile it is considered that all the DG units exchange information with the remaining, defining the consensus matrix to be equal to $C = [c_{mn}] = 1/3, \forall(n,m)\in\mathcal{V}$, as explained in Sec. III-A.

The first iterations for this simple case are shown in Table III. For $k = 0$, all the DG units define the local estimation of the incremental cost as $\lambda_1(0) = \lambda_2(0) = \lambda_3(0) = 0$. To define $P^{G_0}_m(0)$, each DG unit solves the problem in (14). This can be solved analytically, giving the next expression,

$$P^{G_0}_m(k) = \begin{cases} \underline{P}^G_m & \text{if } (\lambda_m(k)-\beta_m)/(2\gamma_m) < \underline{P}^G_m, \\ \overline{P}^G_m & \text{if } (\lambda_m(k)-\beta_m)/(2\gamma_m) > \overline{P}^G_m, \\ \dfrac{\lambda_m(k)-\beta_m}{2\gamma_m} & \text{Otherwise.} \end{cases} \quad (34)$$

Thus, using the current local estimation of $\lambda_m(k)$ and (34), each DG unit defines its optimal active power as $P^{G_0}_1(0) = 40$, $P^{G_0}_2(0) = 20$ and $P^{G_0}_3(0) = 25$, which corresponds to their minimum active power generation. Notice in Table III, that as the unit G_3 operates in PCM, its output power can be defined to be its scheduled value, i. e., $P^{G_0}_3(0) = P^G_3(0) = 25$. For the

This article has been accepted for publication in a future issue of this journal, but has not been fully edited. Content may change prior to final publication. Citation information: DOI 10.1109/TSG.2018.2820748, IEEE Transactions on Smart Grid

units in VCM, the DG current output power can be obtained using power flow models or analytic solutions, if the size of the problem allows it. For real operation, the estimation of the current output power is based on local real-time measurements. In this case, the current output power of the units in VCM can be estimated as[2],

$$P_1^G(k) = \frac{(P^D - P_3^G(k))D_2^P(k)}{D_1^P(k) + D_2^P(k)}, \tag{35}$$

$$P_2^G(k) = \frac{(P^D - P_3^G(k))D_1^P(k)}{D_1^P(k) + D_2^P(k)}. \tag{36}$$

Using these expressions, for $k = 0$, the current output power of the units in VCM are given by $P_1^G(0) = 250$ and $P_2^G(0) = 125$. Additionally, $D_1^P(0)$ and $D_2^P(0)$, are defined as using the standard expression, which is given in (20), defining the values[3] of $D_1^P(0) = 1.57$ and $D_2^P(0) = 3.14$.

For $k = 1$, first all the DG units update their local estimation of the incremental cost, using the expression in (15). For the unit G_1, (15) gives[4],

$$\lambda_1(1) = 1/3\ \lambda_1(0) + 1/3\ \lambda_2(0) + 1/3\ \lambda_3(0) + 33.33(P_1^G(0) - P_1^{G_0}(0)) = 7.00. \tag{37}$$

The factor 33.33 represents κ, calculated as explained in Sec. III-E. For the remaining DG units, the same procedure is done, giving: $\lambda_2(1) = 3.5$ and $\lambda_3(1) = 0$. Once the local estimation of the incremental cost are obtained, each DG unit uses the expression in (34) to obtain their optimal schedule, which gives: $P_1^{G_0}(1) = 40$, $P_2^{G_0}(1) = 20$ and $P_3^{G_0}(1) = 25$. Then, the droop gains of units in VCM are updated, using the expression in (16), giving,

$$D_1^P(1) = D_1^P(0) + 0.0033(P_1^G(0) - P_1^{G_0}(0)) = 1.5707 \tag{38}$$

The factor 0.0033 represents ε. Applying the same procedure for G_2, gives $D_2^P(1) = 3.1404$. Finally, the current output power of the units in VCM are estimated using the expressions in (35) and (36), which gives: $P_1^G(1) = 249.97$ and $P_2^G(1) = 125.03$. Notice in Table III, and as described in Sec. III-B, the units in VCM always maintain the power balance, supplying the total amount of load, even during the execution of the proposed distributed strategy.

This procedure can be applied iteratively, reducing the total generation cost, as can be seen in Table III. The final solution will converge to the optimal solution of the centralized problem, given by $P_1^{G_0} = 193.47$, $P_2^{G_0} = 77.49$ and $P_3^{G_0} = 129.03$, with a total generation cost of 15572.25 \$.

C. Case I: Initialization, Validation and Comparison

Fig. 7 shows the total generation cost, while Fig. 8 and Fig. 9 show the local estimation of the incremental cost variable (λ_m) and the total active output power of each DG unit, respectively; all during operation. The iteration counter

[2]A detailed derivation of this solution can be found in [20].

[3]$D_1^P(0) = 2\pi \cdot 0.1/0.4 = 1.5700$.

[4]In all the protocols, the active power is in p.u., using 1000 kW as the nominal base

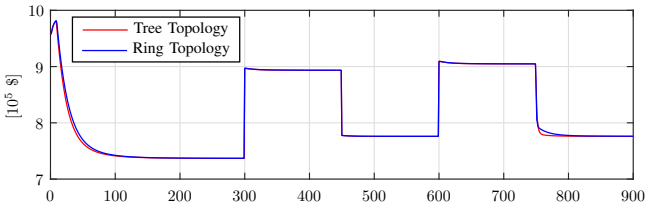

Figure 7. Total generation cost of the DG units considering the ring and tree topology shown in Fig. 5. The x-axis represents k, i.e., the iteration counter.

k, in Fig. 7 to Fig. 9 (and the remaining ones), should be seen as a discretization of the operational time, using a time length of Δt_D (see Sec. IV-F). Additionally, it is assumed that there is not changes in the operational conditions (increase/decrease of load and WT generation) until the proposed strategy reaches the optimal solution. This is done in order to assess its convergence properties.

Initially, the value of λ_m was set to zero at each DG unit. Due to this, the output power of units in PCM is set at their minimum value, as a result of the problem stated in (14). This is shown in the early iterations in Fig. 9d. Simultaneously, the units operating in VCM correct the active power mismatch, supplying the remaining active power, as can be seen in Fig 9a to Fig 9c. After some iterations, the units operating in VCM increase their local estimation of λ_m, as shown in Fig. 8, this value is then distributed through the communication topology, and as a consequence, the output powers of units operating in PCM is increased. The units operating in VCM decrease their output powers to respond to the increase in the output powers of the units operating in PCM. For this, the active gain of the droop loops are modified as shown in Fig. 10. Moreover, due to the way the consensus protocol is defined in (15) for units operating in VCM, their output powers will converge to the optimal value defined through the solution of (14). Therefore, through this cooperative procedure, the total generation cost is reduced as the strategy reaches the optimal solution, as can be seen in Fig. 7.

Regarding the reactive power, as all units operate with a droop-based loop, the reactive generation is distributed proportionally according to the rating of each DG unit, as shown in Fig. 11. Notice that, although the reactive power dispatch is not considered in the proposed strategy, the voltage constraints are considered through the definition of the reactive droop gain in (19), which guarantees that the voltage in the microgrid will operate within the maximum and minimum allowed values, as it is shown in Fig. 12, before and after the convergence of the iteration process. As for the frequency, Fig. 13 compares the frequency of the system with and without considering the protocol in (17). Thus, when protocol in (17) is considered, the system operates with a lower frequency deviation. This is accomplished after each DG unit defines locally their frequency reference ω_m, using local measurements of the system's frequency, as shown also in Fig. 13.

The solution that the proposed distributed strategy reaches is independent of the communication topology of the DG units. This can be seen in Fig. 7, where the total cost is the same for both communication topologies. Moreover, notice that, although the results for the dual variables displayed in Fig. 8 are obtained considering the ring topology shown in

This article has been accepted for publication in a future issue of this journal, but has not been fully edited. Content may change prior to final publication. Citation information: DOI 10.1109/TSG.2018.2820748, IEEE Transactions on Smart Grid

Table III
FIRST ITERATIONS OF THE NUMERICAL EXAMPLE

k	$P_1^G(k)$	$P_2^G(k)$	$P_3^G(k)$	$\sum P_m^G(k)$	$D_1^P(k)$	$D_2^P(k)$	$\lambda_1(k)$	$\lambda_2(k)$	$\lambda_3(k)$	$P_1^{G_0}(k)$	$P_2^{G_0}(k)$	$P_3^{G_0}(k)$	\$
0	250.00	125.00	25.00	400.0	1.5700	3.1400	0.000	0.000	0.000	40.00	20.00	25.00	20586.75
1	249.97	125.03	25.00	400.0	1.5707	3.1404	7.000	3.500	0.000	40.00	20.00	25.00	20587.44
2	249.94	125.06	25.00	400.0	1.5714	3.1407	10.499	7.001	3.500	40.00	20.00	25.00	20588.14
3	249.92	125.08	25.00	400.0	1.5721	3.1411	13.998	10.502	7.000	40.00	20.00	25.00	20588.83
4	249.89	125.11	25.00	400.0	1.5728	3.1414	17.497	14.003	10.500	43.12	20.00	25.00	20589.53
5	249.86	125.14	25.00	400.0	1.5735	3.1418	20.892	17.504	14.000	51.61	20.00	25.00	20590.21
6	247.34	123.92	28.74	400.0	1.5741	3.1421	24.074	20.970	17.465	59.56	20.82	28.74	20247.74
7	243.58	122.06	34.36	400.0	1.5748	3.1424	27.096	24.273	20.836	67.11	24.12	34.36	19756.54
8	239.97	120.29	39.75	400.0	1.5754	3.1428	29.950	27.333	24.068	74.25	27.18	39.75	19311.92
9	236.56	118.61	44.83	400.0	1.5759	3.1431	32.641	30.221	27.117	80.98	30.07	44.83	18916.08
10	233.35	117.03	49.62	400.0	1.5764	3.1434	35.179	32.944	29.993	87.32	32.79	49.62	18563.74

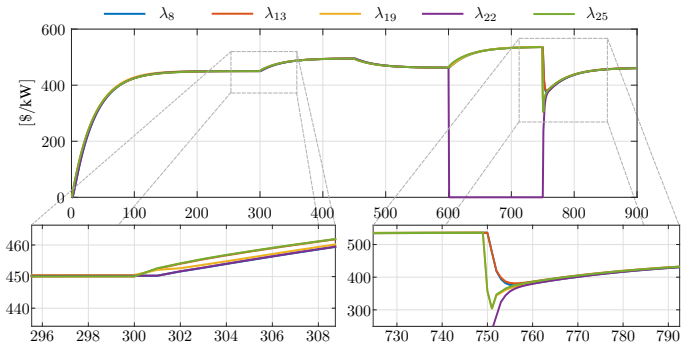

Figure 8. Local estimation of the incremental cost variable (or dual variable) at each DG unit using the ring topology in Fig.5*b*. The x-axis represents k, i.e., the iteration counter.

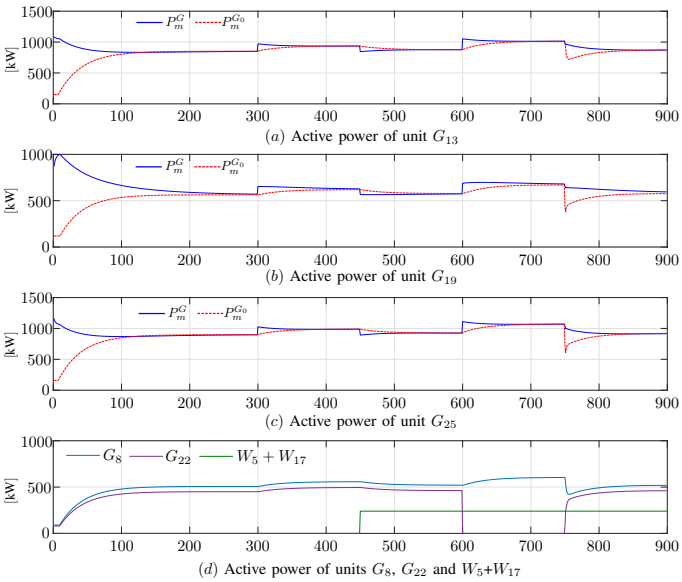

Figure 9. Total active output power of DG and WT units. The x-axis represents k, i.e., the iteration counter. In (a) to (c), the blue line represents P_m^G, i.e., the real active power of the DG units, while the dashed red line represents $P_m^{G_0}$, i.e., the optimal scheduled active power of each DG unit. After convergence, the real output and the optimal scheduled power are the same.

Fig. 5*b*, the same results are obtained if the tree topology is considered instead. In this sense, the main difference is related to the speed of convergence of the consensus algorithm, which depends on the connectivity (i.e., the number of links) of the communication topology.

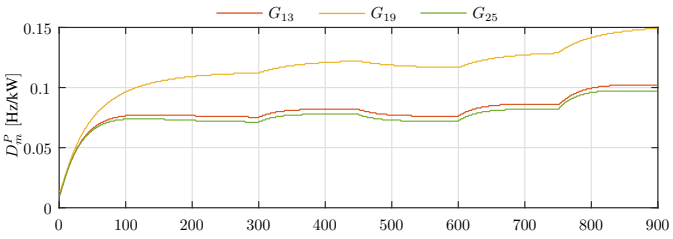

Figure 10. Active droop gain of units operating in VCM during operation. The x-axis represents k, i.e., the iteration counter.

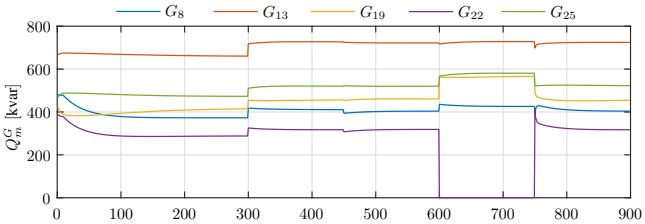

Figure 11. Total reactive output power of all the DG units. The x-axis represents k, i.e., the iteration counter.

Notice that the formulation of the optimal generation problem in Sec. II-B is independent on the operational mode of the DG units (VCM or PCM), suggesting that the optimal solution is also independent on these operation modes. However, as units operating in VCM share the power losses in proportion to the their ratings, the final solution will depend on the set of units operating in VCM and in PCM. To show this, Table IV compares the optimal solution for different cases of modes of operation. In all cases, the communication topology used was the ring topology. According to these results, the solution obtained have the same total generation cost, but different active power losses and incremental cost variable. The same total generation cost is due to the cost of the power losses, which is negligible when compared with the cost of supplying the total active load consumption.

The selection of the units operating in VCM is an important issue, as these units are responsible for automatically correct the mismatch between generation and load consumption after any change in the operating conditions and, more importantly, during the optimization process. Therefore, its selection should be based on their maximum generation capacity. In this context, if the generation capacity of these units is lower than the total load demand, the droop control cannot guarantee

This article has been accepted for publication in a future issue of this journal, but has not been fully edited. Content may change prior to final publication. Citation information: DOI 10.1109/TSG.2018.2820748, IEEE Transactions on Smart Grid

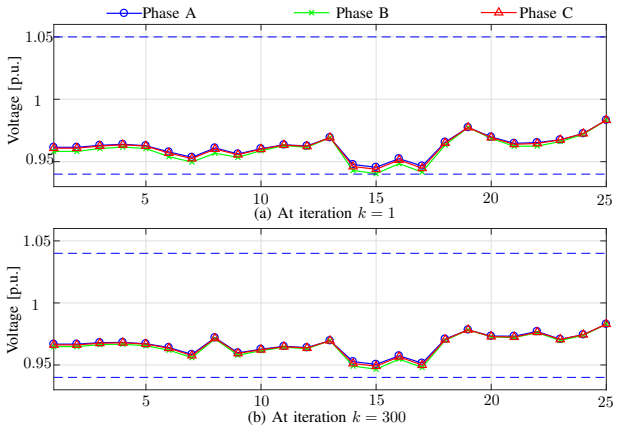

Figure 12. Voltage profile of the microgrid for all the phases before and after the convergence process.

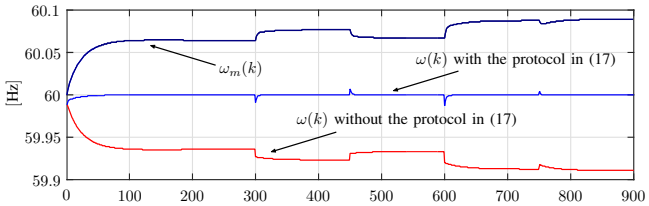

Figure 13. Frequency and frequency reference for all units during operation. The x-axis represents k, i.e., the iteration counter.

a feasible operation, especially in the early iterations of the optimization process and after any load increase or WT generation reduction.

Table IV also shows a comparison with the solution obtained using the centralized strategy in [33], which considers a static droop operation framework, i.e., the active and reactive droop gains are not modified during operation, and they are defined based on the Standard IEEE 1547.7 [34]. In this case, as the strategy proposed in [33] is centralized, all the information regarding the microgrid, the DG units and loads is available in advance, gathered by a high-level and central operator. According to these results, the total generation cost and the power losses are reduced 0.6% and 2.4%, when comparing the distributed with the centralized solution. Notice that the static definition for the active droop gain (D_m^P) used by the centralized solution does not consider the economic operation of the DG units, but only the generation capacity instead, sharing the active load among all the units in proportion to their ratings [33]. In contrast, the proposed approach defines the active droop gains based on the solution of the economical dispatch problem, and consequently, a lower cost solution is obtained. Regarding the frequency, the microgrid operates with the nominal value in steady-state in all cases, while in the solution obtained by the centralized strategy a deviation of 0.05% was observed. These results show the effectiveness of the proposed strategy when compared with a centralized strategy.

D. Case II: Time-varying Conditions

To assess the flexibility of the proposed distributed strategy under time-varying conditions, different unexpected changes in the operational conditions of the microgrid are analyzed. Here, the communication topology used was also the ring topology. At $k = 300$, the load demand is increased by 10%. In this

Table IV
COMPARISON OF THE DISTRIBUTED STRATEGY FOR DIFFERENT CASES

	Distributed Strategy			Centralized [33]
Units in PCM	G_8, G_{22}	G_8	–	–
Units in VCM	G_{13}, G_{19} G_{25}	G_{13}, G_{19}, G_{22}, G_{25}	G_8, G_{13}, G_{19}, G_{22}, G_{25}	G_8, G_{13}, G_{19}, G_{22}, G_{25}
Total Cost [10^5\$]	7.369	7.369	7.369	7.413
Total Losses [kW]	32.77	32.79	33.04	33.54
Frequency [Hz]	60.00	60.00	60.00	59.97
$\max\{\lambda_m\}$ [\$/kW]	450.495	450.43	450.328	–
$\min\{\lambda_m\}$ [\$/kW]	450.058	450.095	450.185	–
$\min\{V_{m,\phi}\}$ [*p.u.*]	0.9466	0.9460	0.9430	0.9430

case, units operating in VCM respond automatically correcting the active power mismatch in the EDS, as can be seen in Fig 9. Due to this, the local estimation of the incremental cost variable (λ_m) are increased, which cause that units in PCM respond to the new operational condition, increasing their output active powers. After some iterations, the system reaches a new optimal operational state. At $k = 450$, both WTs are dispatched, as shown in Fig 9d. This increase in the renewable generation creates an active power mismatch (generation is higher than consumption), causing that units operating in VCM respond automatically and reaching a new operational condition characterized by a lower value of the incremental cost variable, as shown in Fig 8.

At $k = 600$, unit G_{22}, which is operating in PCM, unexpectedly is turned off and all its communication links are disabled, simulating a fault. Here, it is assumed that the WTs generation maintains the same value in order to assess only the impact due to the DG units fault. This fault creates an active power mismatch (generation is lower than consumption), that leads to an immediate response of the units operating in VCM. In fact, this is one of the main advantages of the proposed strategy, since some units operate in VCM mode (i.e., with an active droop loop), they are responsible for automatically reduce the active power mismatch between generation and consumption after any change in the operational conditions of the microgrid, using only local information, increasing the robustness and reliability during operation.

Finally, at $k = 750$, unit G_{22} restores its operation and the system reaches the same optimal operational point before the fault. Notice, however, after unit G_{22} is turned on, the units operating in VCM have a different value of active droop gains, as shown in Fig. 10. This is due to the fact that the output power of units operating in VCM, defined through the active droop loops, depends on the rates $D_m^G/D_n^G, \forall m, n \in \mathcal{G}_2$, which in this case are the same before and after the simulated fault of unit G_{22}.

E. Case III: Impact of the Communication Topology on the Performance

In this section, the impact of the communication topology on the performance of the proposed strategy is assessed. To do this, the communication topologies shown in Fig. 14 are considered, in addition to the ring and tree topologies shown in Fig. 5. All the parameters, units operating in VCM and PCM, are defined as in Case I.

This article has been accepted for publication in a future issue of this journal, but has not been fully edited. Content may change prior to final publication. Citation information: DOI 10.1109/TSG.2018.2820748, IEEE Transactions on Smart Grid

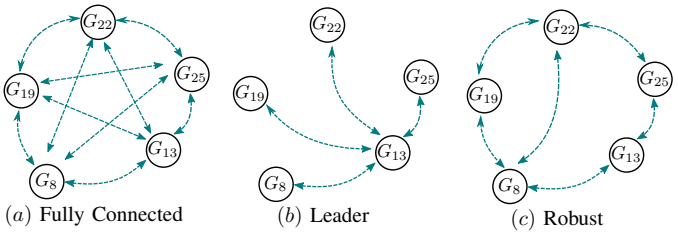

Figure 14. Additional communication topologies used to test the proposed strategy. The robust topology was designed using the rule proposed in [12].

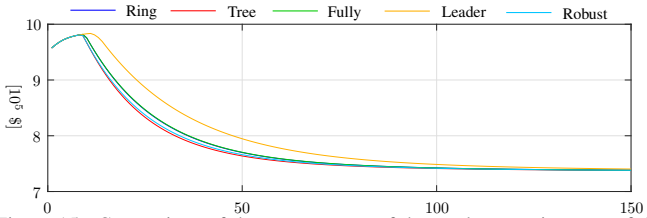

Figure 15. Comparison of the convergence of the total generation cost of the DG units for different communication topologies. The x-axis represents k, i.e., the iteration counter.

The convergence of the proposed strategy can be affected by the connectivity level of the DG units, as it is based on a first-order consensus algorithm. This level of connectivity can be measured by the coefficient β, defined by the relationship between the number of links over the number of DG units. For the considered topologies, this takes the value of 1 and 0.8 for the ring and tree topologies, respectively (see Fig. 5); and 2, 0.8 and 1.2 for the fully connected, leader and robust topologies, respectively (see Fig. 14). Thus, it is expected that communication topologies with higher value of β, reach consensus faster. However, according to the results shown in Fig. 15, the tree and robust topology have better performance (i.e., they converge faster) when compared with the fully connected topology, which has the higher β. Considering these results, it is possible to conclude that although the level of connectivity β and the speed of convergence are closely related, there is no an inversely proportional relationship between them. For this reason, it is not possible to know exactly which topology will have the fastest convergence speed based exclusively on the values of β. These results are in agreement with those presented in [7], where a first-order consensus algorithm was also studied. Finally, it is important to add that in the simulations the proposed strategy defines the same optimal dispatch for all the DG units, regardless the communication topology used.

F. Case IV: Scalability and Computational Time

In this section, simulations with 3, 7 and 10 DG units were carried out, in addition to the case with 5 DG units presented in Sec. IV-C. This is done in order to assess the scalability performance of the proposed strategy. In all the simulations, the communication topology used was the ring topology, while the units operating in VCM and PCM are selected following the discussion presented in Sec. IV-C.

Fig. 16 shows the active output power of the DG units in VCM and PCM in all cases. For these simulations, the maximum computational time required by one DG unit to solve the problem (14) in one iteration k, is near to 0.030 s. Based on this, a conservative value of 0.1 s can be used as the time-step to discretize the operational time (Δt_D). This time should also include the time to perform all the measurements and exchange the data between the DG units. In this context, this low computational time is one of the main advantages of the proposed distributed strategy, which is a consequence of the reduction of the size of the optimization problem solved by each DG unit. Notice that in all cases, all the DG units have reached consensus in less than 400 iterations, which means that the proposed approach requires approximately 12 s to converge to the optimal solution (or 40 s, if 0.1 s is used for Δt_D), if all the DG units execute the optimization process in parallel, as expected in practical implementations. In fact, based on the hierarchical control approach discussed in Sec. III-D, the maximum time for the distributed approach to reach the optimal solution is actually limited by $\mathcal{T}_D$, which can take values in the order of minutes. Thus, the proposed algorithm is sufficiently fast and suitable for implementation.

Finally, it is important to highlight that the results shown in Fig. 16 were obtained using the proposed heuristic rules in (18), showing their good performance for these cases, as the distributed strategy properly reaches the optimal solution.

V. Conclusion

In this paper, a distributed strategy for optimal dispatch of unbalanced three-phase islanded microgrids was presented. To define the generation dispatch of the DG units that minimize the overall generation cost, an optimization problem is stated and solved distributively based on primal-dual constrained decomposition and a first-order consensus algorithm. Two operational modes are considered for the DG units: VCM and PCM. Comprehensive simulations and comparison were given to show the effectiveness and flexibility of the proposed distributed approach.

According to the obtained results, the proposed strategy achieves a lower cost solution, when compared with the standard centralized approach based on a static droop framework, since the solution of the economic dispatch is used to define the active droop gains; while the frequency deviation is reduced in steady-state, using a local correction term. Additionally, as units in VCM operate with an active droop loop, they are responsible for automatically reduce the active power mismatch between the generation and the consumption, after any change in the operational conditions of the microgrid and, more importantly, during the optimization process. Finally, as the proposed strategy is considered to operate within the standard hierarchical control framework, the dynamics of the primary level (implemented with droop control) and the dispatch layer (implemented in the Stage I and II) are decoupled, which helps to maintain the stability of the system.

Appendix
Convergence Analysis of the Proposed Distributed Strategy

To study the convergence of the proposed distributed strategy, the next conditions are assumed to hold,

(C1) Condition 1: The problem in (4)–(6) is technically feasible i. e., the DG units in VCM have enough generation

This article has been accepted for publication in a future issue of this journal, but has not been fully edited. Content may change prior to final publication. Citation information: DOI 10.1109/TSG.2018.2820748, IEEE Transactions on Smart Grid

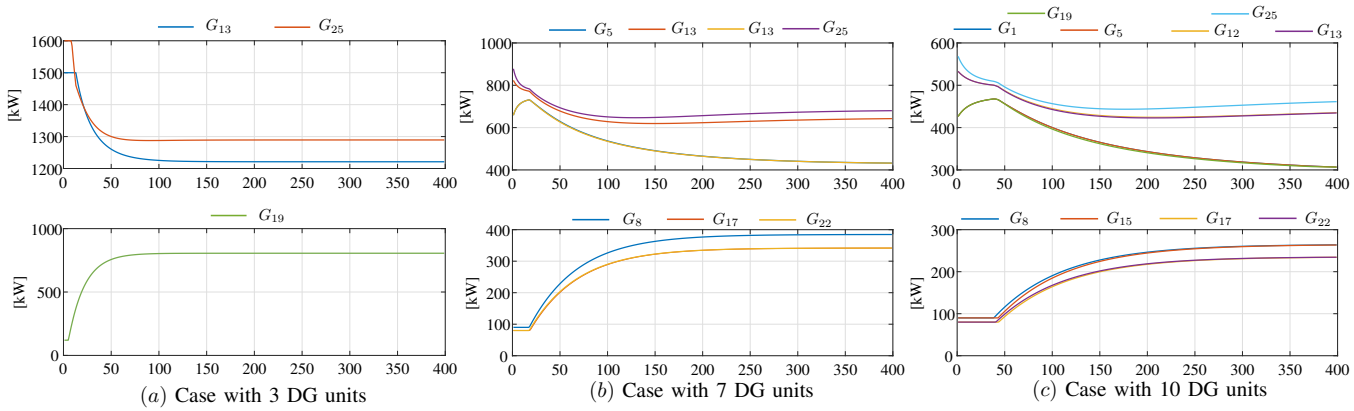

(a) Case with 3 DG units (b) Case with 7 DG units (c) Case with 10 DG units

Figure 16. Active output power of the DG units for the cases with 3, 7 and 10 units. Upper: Units in VCM. Lower: Units in PCM. The x-axis represents k, i.e., the iteration counter.

capacity to correct the active power mismatch between generation and consumption during the optimization process. This can be written mathematically as,

$$\sum_{m\in\mathcal{G}_2} \overline{P}_m^G \gg \sum_{m\in\mathcal{N}} \sum_{\phi\in\mathcal{F}} P_{m,\phi}^D - \sum_{m\in\mathcal{W}} P_m^W. \tag{39}$$

(C2) Condition 2: All the DG units exchange information following a pre-defined communication topology, which defines the consensus matrix $C = [c_{mn}]$, designed as explained in Sec. III-E.

(C3) Condition 3: All the DG units gather the required data, process and update their protocols synchronously and in parallel.

Thus, the next proposition can be defined,

(P1) Proposition 1: The proposed distributed strategy converge monotonically if conditions C1–C3 holds.

To prove Proposition 1, first, recall the proposed distributed strategy.

For each iteration k, and each DG unit $m \in \mathcal{G}$, apply sequentially:

$$P_m^{G_0}(k) = \arg\min_{P_m^G\in\mathcal{O}_m} \left[f_m(P_m^{G_0}) - \lambda_m(k) P_m^{G_0} \right] \tag{40}$$

$$\Delta P_m^G(k) = P_m^G - P_m^{G_0}(k) \tag{41}$$

$$\lambda_m(k+1) = \sum_{n\in\mathcal{N}_m} c_{mn}\lambda_n(k) + \kappa \Delta P_m^G(k) \tag{42}$$

$$D_m^P(k+1) = D_m^P(k) + \varepsilon \Delta P_m^G(k) \tag{43}$$

$$\Delta\omega(k+1) = \omega_0 - \omega \tag{44}$$

$$\omega_m(k+1) = \omega_m(k) + \hat{\varepsilon}\Delta\omega(k+1) \tag{45}$$

In (41), P_m^G corresponds to the total active output power of the DG units, meanwhile ω in (44), corresponds to the angular frequency of the microgrid, both obtained by the DG unit through local measurements.

Additionally, consider the next following lemmas,

(L1) Lemma 1: The active output power of a DG unit operating with droop control is inversely proportional to its active droop gain, or equivalently, $P_m^G \propto 1/D_m^P$.

Proof: A technical discussion related to the operation of DG units with droop control is presented in [20].

(L2) Lemma 2: In (40), $P_m^{G_0}(k+1) > P_m^{G_0}(k)$, if $\lambda_m(k+1) > \lambda_m(k)$.

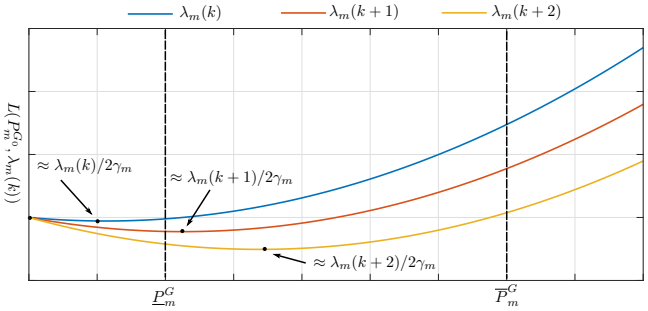

Figure 17. Schematic representation of $L(P_m^{G_0}, \lambda_m(k))$ in (48), as a function of $P_m^{G_0}$ for different values of $\lambda_m(k)$, such that $\lambda_m(k+2) > \lambda_m(k+1) > \lambda_m(k)$. $P_m^{G_0}$ can be obtained as the root of $\partial L(\cdot)$, which is approximately $\approx \lambda_m(k)/2\gamma_m$. The areas, $P_m^G < \underline{P}_m^G$ and $P_m^G > \overline{P}_m^G$, represent the non-feasible values for $P_m^{G_0}$, according to the set $\mathcal{O}_m$.

Proof: Recall that (40) is equivalent to the definition of the Lagrangian given in (12). Thus, (40) can be stated as,

$$L(P_m^{G_0}, \lambda_m(k)) = \gamma_m (P_m^{G_0})^2 + \beta_m P_m^{G_0} + \alpha_m - \lambda_m(k) P_m^{G_0}, \tag{46}$$

which can be re-written as,

$$L(\cdot) = \gamma_m (P_m^{G_0})^2 + (\beta_m - \lambda_m(k)) P_m^{G_0} + \alpha_m. \tag{47}$$

Considering that $\alpha_m = 0$, since the shut-up/shut-down cost is not considered; and $\lambda_m(k) \gg \beta_m$ in the economic dispatch problem [35], (47) can be approximated as,

$$L(\cdot) \approx \gamma_m (P_m^{G_0})^2 - \lambda_m(k) P_m^{G_0}. \tag{48}$$

In order to better understand the solution of (40), which defines $P_m^{G_0}$, as a function of $\lambda_m(k)$, Fig. 17 shows the second-order polynomial function given by (48), for different values of $\lambda_m(k)$. Notice that the solution of (40) is equivalent to find the root of the derivative of (48), in such a way that $P_m^{G_0} \in \mathcal{O}_m$. This root can be analytically found as,

$$\frac{\partial L(\cdot)}{\partial P_m^{G_0}} = 2\gamma_m P_m^{G_0} - \lambda_m(k) = 0, \tag{49}$$

which gives that,

$$P_m^{G_0} \approx \left[\lambda_m(k)/2\gamma_m \right]_{P_m^{G_0}\in\mathcal{O}_m}. \tag{50}$$

Thus, as $\gamma_m > 0$, from (50) and Fig. 17, is possible to conclude that $P_m^{G_0} \propto \lambda_m(k)$, which prove L2.

For each iteration $k \in \mathbb{Z}^+ \cup \{0\}$, let construct the series of variables $(\Delta P_m^G, \lambda_m(k), P_m^{G_0}(k), D_m^P(k), \Delta\omega(k), \omega_m(k))$, following the iterative strategy in (41)–(45). Proposition 1 will be proved, if the series defined using (41)–(45) converge and are monotonic. To show this, let $k = 0$, thus $\lambda_m(0) = 0, \forall m \in \mathcal{G}$, while $D_m^P(0)$ is defined as in (20) and $\omega_m(0) = \omega_0$, as explained in Sec. IV. Since $\lambda_m(0) = 0$, then $P_m^{G_0}(0) = \underline{P}_m^G$, due to (50). Moreover, $P_m^G > 0$, since C1 holds and the DG units in VCM correct the active power mismatch in the microgrid. Thus, $\Delta P_m^G(0) > 0$.

For $k = 1$, $\lambda_m(1) > \lambda_m(0)$ and $D_m^P(1) > D_m^P(0)$, since $\Delta P_m^G(0) > 0$ and $\kappa > 0, \epsilon > 0$ in (42) and (43). As $\lambda_m(1) > \lambda_m(0)$, then, $P_m^{G_0}(1) > P_m^{G_0}(0)$ in (40) and due to L2. Moreover, $P_m^G(1) < P_m^G(0)$ since $D_m^P(1) > D_m^P(0)$ and due to L1. Finally, $\Delta\omega(1) > 0$, since in islanded droop-based microgrids, the frequency is under the nominal value when the frequency reference is set to ω_0 [33], as for $k = 0$. Thus, $\omega_m(1) > \omega_m(0)$, since $\hat{\epsilon} > 0$, and as a consequence, $\Delta\omega_m(1) < \Delta\omega(0)$, which means that deviation of the frequency of the microgrid is reduced, considering also that C3 holds (see in Fig. 1 ω when ω_m increase).

Because of the iterative nature of (41)–(45), it can be verified that the following monotonic series exits for $k = 2, 3, 4, ...,$

$$\begin{aligned}
&\{P_m^G(k)\} : P_m^G(0) > P_m^G(1) > \cdots > \underline{P}_m^G \\
&\{P_m^{G_0}(k)\} : P_m^{G_0}(0) < P_m^{G_0}(1) < \cdots < \overline{P}_m^G \\
&\{\Delta P_m^G(k)\} : \Delta P_m^G(0) > \Delta P_m^G(1) > \cdots > 0 \\
&\{\lambda_m(k)\} : \lambda_m(0) < \lambda_m(1) < \cdots < \lambda \\
&\{D_m^P(k)\} : D_m^P(0) < D_m^P(1) < \cdots < D_m^P(k) \\
&\{\Delta\omega(k)\} : \Delta\omega(0) > \Delta\omega(1) > \cdots > 0 \\
&\{\omega_m(k)\} : \omega_m(0) < \omega_m(1) < \cdots < \omega_m(k).
\end{aligned}$$

In the last series, $\underline{P}_m^G$ is a bound of $\{P_m^G(k)\}$, while $\overline{P}_m^G$ is a bound of $\{P_m^{G_0}(k)\}$. Moreover, the series $\{P_m^G(k)\}$ is monotonically decreasing, while the series $\{P_m^{G_0}(k)\}$ is monotonically increasing. Due this, the series $\{\Delta P_m^G(k)\}$ is monotonically decreasing and bounded by 0. These series can be technically interpreted as, during the optimization process, the DG units can not supply lower than $\underline{P}_m^G$ and the optimal dispatch can not be greater than $\overline{P}_m^G$. The fact that the series $\{\Delta P_m^G(k)\}$ is decreasing imply that P_m^G converge to $P_m^{G_0}$.

The series $\{\lambda_m(k)\}$, $\{D_m^P(k)\}$ and $\{\omega_m(k)\}$ are not bounded, but they are limited since their definition in (42), (43) and (45), are a function of $\Delta P_m^G(k)$ and $\Delta\omega(k)$, which are bounded and monotonically converge to 0. Additionally, as C2 holds, all the $\lambda_m(k)$ converge to λ through the consensus matrix $C = [c_{mn}]$.

Thus, based on the fact that as all these series are monotonic and limited, P1 is proved to be valid.

REFERENCES

[1] J. Zhu, *Optimization of Power System Operation*. USA: Wiley-IEEE, 2009.

[2] D. Olivares, C. Cañizares, and M. Kazerani, "A centralized energy management system for isolated microgrids," *IEEE Trans. Smart Grid*, vol. 5, no. 4, pp. 1864–1875, July 2014.

[3] K. H. Youssef, "Power quality constrained optimal management of unbalanced smart microgrids during scheduled multiple transitions between grid-connected and islanded modes," *IEEE Trans. Smart Grid*, vol. 8, no. 1, pp. 457–464, Jan. 2017.

[4] P. P. Vergara, J. C. Lopez, L. C. da Silva, and M. J. Rider, "Security-constrained optimal energy management system for three-phase residential microgrids," *Electr. Pow. Syst. Res.*, vol. 146, pp. 371–382, May 2017.

[5] W. Shi, X. Xie, C. C. Chu, and R. Gadh, "Distributed optimal energy management in microgrids," in *IEEE Trans. Smart Grid*, vol. 6, no. 3, May 2015, pp. 1137–1146.

[6] Y. Wang, S. Wang, and L. Wu, "Distributed optimization approaches for emerging power systems operation: A review," *Electr. Pow. Syst. Res.*, vol. 144, pp. 127 – 135, 2017.

[7] Z. Zhang and M. Y. Chow, "Convergence analysis of the incremental cost consensus algorithm under different communication network topologies in a smart grid," *IEEE Trans. Power Systems*, vol. 27, no. 4, pp. 1761–1768, Nov. 2012.

[8] S. Yang, S. Tan, and J. X. Xu, "Consensus based approach for economic dispatch problem in a smart grid," *IEEE Trans. Power Systems*, vol. 28, no. 4, pp. 4416–4426, Nov 2013.

[9] G. Hug, S. Kar, and C. Wu, "Consensus and innovations approach for distributed multiagent coordination in a microgrid," *IEEE Trans. Smart Grid*, vol. 6, no. 4, pp. 1893–1903, July 2015.

[10] G. Chen, J. Ren, and E. N. Feng, "Distributed finite-time economic dispatch of a network of energy resources," *IEEE Trans. Smart Grid*, to be published, 2016.

[11] F. Guo, C. Wen, J. Mao, and Y. D. Song, "Distributed economic dispatch for smart grids with random wind power," *IEEE Trans. Smart Grid*, vol. 7, no. 3, pp. 1572–1583, May 2016.

[12] W. Zhang, W. Liu, X. Wang, L. Liu, and F. Ferrese, "Online optimal generation control based on constrained distributed gradient algorithm," *IEEE Trans. Power Systems*, vol. 30, no. 1, pp. 35–45, Jan 2015.

[13] R. Mudumbai, S. Dasgupta, and B. B. Cho, "Distributed control for optimal economic dispatch of a network of heterogeneous power generators," *IEEE Trans. Power Systems*, vol. 27, no. 4, pp. 1750–1760, Nov 2012.

[14] G. Binetti, A. Davoudi, F. L. Lewis, D. Naso, and B. Turchiano, "Distributed consensus-based economic dispatch with transmission losses," *IEEE Trans. Power Systems*, vol. 29, no. 4, pp. 1711–1720, July 2014.

[15] Y. Xu and Z. Li, "Distributed optimal resource management based on the consensus algorithm in a microgrid," *IEEE Trans. on Ind. Electr.*, vol. 62, no. 4, pp. 2584–2592, April 2015.

[16] G. Chen, F. L. Lewis, E. N. Feng, and Y. Song, "Distributed optimal active power control of multiple generation systems," *IEEE Trans. Ind. Electr.*, vol. 62, no. 11, pp. 7079–7090, Nov 2015.

[17] H. Pourbabak, J. Luo, T. Chen, and W. Su, "A novel consensus-based distributed algorithm for economic dispatch based on local estimation of power mismatch," *IEEE Trans. Smart Grid*, to be published, 2017.

[18] J. M. Guerrero, J. C. Vasquez, J. Matas, L. G. de Vicuña, and M. Castilla, "Hierarchical control of droop-controlled AC and DC microgrids - A general approach toward standardization," *IEEE Trans. Ind. Electron.*, vol. 58, no. 1, pp. 158–172, Jan. 2011.

[19] W. J. Ma, J. Wang, V. Gupta, and C. Chen, "Distributed energy management for networked microgrids using online alternating direction method of multipliers with regret," *IEEE Trans. Smart Grid*, to be published, 2016.

[20] S. J. Ahn, J. W. Park, I. Y. Chung, S. I. Moon, S. H. Kang, and S. R. Nam, "Power-sharing method of multiple distributed generators considering control modes and configurations of a microgrid," *IEEE Trans. Power Delivery*, vol. 25, no. 3, pp. 2007–2016, July 2010.

[21] D. Wu, F. Tang, T. Dragicevic, J. C. Vasquez, and J. M. Guerrero, "A control architecture to coordinate renewable energy sources and energy storage systems in islanded microgrids," *IEEE Trans. Smart Grid*, vol. 6, no. 3, pp. 1156–1166, May 2015.

[22] J. Matas, M. Castilla, L. G. d. Vicuña, J. Miret, and J. C. Vasquez, "Virtual impedance loop for droop-controlled single-phase parallel inverters using a second-order general-integrator scheme," *IEEE Trans. Power Electronics*, vol. 25, no. 12, pp. 2993–3002, Dec 2010.

[23] J. M. Rey, P. Marti, M. Velasco, J. Miret, and M. Castilla, "Secondary switched control with no communications for islanded microgrids," *IEEE Trans. Ind. Electronics*, vol. 64, no. 11, pp. 8534–8545, Nov. 2017.

[24] R. Olfati-Saber and R. M. Murray, "Consensus problems in networks of agents with switching topology and time-delays," *IEEE Trans. Automatic Control*, vol. 49, no. 9, pp. 1520–1533, Sep. 2004.
[25] R. Olfati-Saber, J. A. Fax, and R. M. Murray, "Consensus and cooperation in networked multi-agent systems," *Proceedings of the IEEE*, vol. 95, no. 1, pp. 215–233, Jan 2007.
[26] M. Zhu and S. Martinez, "On distributed convex optimization under inequality and equality constraints," *IEEE Trans. Automatic Control*, vol. 57, no. 1, pp. 151–164, Jan. 2012.
[27] F. Chen, M. Chen, Q. Li, K. Meng, Y. Zheng, J. M. Guerrero, and D. Abbott, "Cost-based droop schemes for economic dispatch in islanded microgrids," *IEEE Trans. Smart Grid*, vol. 8, no. 1, pp. 63–74, Jan. 2017.
[28] Q. Shafiee, C. Stefanovic, T. Dragicevic, P. Popovski, J. C. Vasquez, and J. M. Guerrero, "Robust networked control scheme for distributed secondary control of islanded microgrids," *IEEE Trans. Ind. Electronics*, vol. 61, no. 10, pp. 5363–5374, Oct 2014.
[29] X. Lu, X. Yu, J. Lai, Y. Wang, and J. M. Guerrero, "A novel distributed secondary coordination control approach for islanded microgrids," *IEEE Trans. Smart Grid*, to be published, 2017.
[30] M. M. A. Abdelaziz, H. E. Farag, E. F. El-Saadany, and Y. Mohamed, "A novel and generalized three-phase power flow algorithm for islanded microgrids using a newton trust region method," *IEEE Trans. Power Systems*, vol. 28, no. 1, pp. 190–201, Feb. 2013.
[31] A. Wachter and L. T. Biegler, "On the implementation of an interior-point filter line-search algorithm for large-scale nonlinear programming," *Math. Prog.*, vol. 106, no. 1, pp. 25–57, 2006.
[32] G. K. V. Raju and P. R. Bijwe, "Efficient reconfiguration of balanced and unbalanced distribution systems for loss minimisation," *IET Gen. Trans. Distr.*, vol. 2, no. 1, pp. 7–12, Jan. 2008.
[33] P. P. Vergara, J. C. Lopez, M. J. Rider, and L. C. P. da Silva, "Optimal operation of unbalanced three-phase islanded droop-based microgrids," *IEEE Trans. Smart Grid*, to be published, 2017.
[34] *Standard 1547: IEEE Standard for Interconnecting Distributed Resources with Electric Power Systems,*, IEEE Interconnecting Committee Std., 2013.
[35] A. Wood and B. Wollenberg, *Power Generation, Operation and Control*. New York, NY, USA: Wiley, 1996.

Pedro P. Vergara was born in Barranquilla, Colombia in 1990. He received the B.Sc. degree in electronic engineering from the Universidad Industrial de Santander, Bucaramanga, Colombia, in 2012, and the M.Sc. degree in electrical engineering from University of Campinas, UNICAMP, Campinas, Brazil, in 2015. He is currently working toward the Ph.D. degree in electrical engineering at the University of Campinas and at the University of Southern Denmark, SDU, Denmark, as part of a double degree program between UNICAMP and SDU. His current research interests include development of methodologies for the optimization, planning, and control of electrical distribution systems with high penetration of distributed generation and renewable energy systems.

Juan M. Rey was born in Bucaramanga, Colombia in 1989. He received the B.S. in electrical engineering from Universidad Industrial de Santander, Bucaramanga, Colombia, in 2012. He is currently working toward the Ph.D. degree in the Department of Electronic Engineering, Technical University of Catalonia, Spain. Since 2013, he has been with the Electrical, Electronic and Telecommunications Engineering School (E3T), Universidad Industrial de Santander, Bucaramanga Colombia, where he is currently an Assistant Professor. His research interest are power electronics and control for distributed generation and microgrids.

Hamid R. Shaker received his PhD in 2010 from Aalborg University, Denmark. He has been a visiting researcher at MIT, a post-doctoral researcher and an assistant professor at Aalborg University within 2009-2013 and an associate professor at Norwegian University of Science and Technology (NTNU), Norway within 2013-2014. Since 2014, he has been an associate professor at Center for Energy Informatics, University of Southern Denmark. His research interests are in the area of fault detection and diagnosis, processes monitoring, modeling and control with applications in energy technology. His contributions have been reported in more than 90 journal and conference publications. He serves three journals as a member of editorial board and has been IPC member for several conferences.

Josep M. Guerrero (S'01-M'04-SM'08-FM'15) received the B.S. degree in telecommunications engineering, the M.S. degree in electronics engineering, and the Ph.D. degree in power electronics from the Technical University of Catalonia, Barcelona, in 1997, 2000 and 2003, respectively. Since 2011, he has been a Full Professor with the Department of Energy Technology, Aalborg University, Denmark, where he is responsible for the Microgrid Research Program (www.microgrids.et.aau.dk). His research interests are oriented to different microgrid aspects, including power electronics, distributed energy-storage systems, hierarchical and cooperative control, energy management systems, smart metering and the internet of things for AC/DC microgrid clusters and islanded minigrids.
Prof. Guerrero is an Associate Editor for a number of IEEE TRANSACTIONS. He received the best paper award of the IEEE Transactions on Energy Conversion for the period 2014-2015, and the best paper prize of IEEE-PES in 2015. As well, he received the best paper award of the Journal of Power Electronics in 2016. In 2014, 2015, 2016, and 2017 he was awarded by Thomson Reuters as Highly Cited Researcher, and in 2015 he was elevated as IEEE Fellow for his contributions on distributed power systems and microgrids.

Bo Nørregaard Jørgensen is founder and head of Center for Energy Informatics at the University of Southern Denmark. Center for Energy Informatics is an interdisciplinary research center focusing on innovative solutions for facilitating the transition towards a smart sustainable energy system. The center's research is conducted in close collaboration with industrial partners, public bodies, and government agencies. As head of center, Dr. Jørgensen represent University of Denmark at national and international events, in advisory boards and government reference committees. He is appointed member of the Danish Academy of Technical Science. Dr. Jørgensen research focuses on integration and management of demand-side flexibility with supply-side fluctuations, from the business and technological perspectives. He holds a Ph.D. in Computer Science from the University of Southern Denmark, a M.Sc. and a B.Sc. in Computer System Engineering from Odense University, Denmark.

Luiz C. P. da Silva graduated in electrical engineering in Federal University of Goias, Goias, Brazil, in 1995 and received the M.Sc. and Ph.D. degrees in electrical engineering from the University of Campinas, UNICAMP, Campinas, Brazil, in 1997 and 2001, respectively. From 1999 to 2000, he was visiting Ph.D. student at the University of Alberta, Edmonton, AB, Canada. Currently, he is an Associate Professor at the University of Campinas, UNICAMP, Campinas, Brazil. His research interests are power system transmission and distribution.